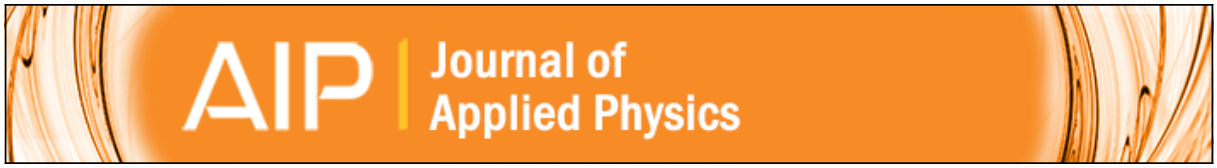

Ab initio design of coherent thermal sources

Jérémie Drevillon and Philippe Ben-Abdallah

Citation: Journal of Applied Physics **102**, 114305 (2007); doi: 10.1063/1.2816244
View online: http://dx.doi.org/10.1063/1.2816244
View Table of Contents: http://scitation.aip.org/content/aip/journal/jap/102/11?ver=pdfcov
Published by the AIP Publishing

Articles you may be interested in

Micromachined single-level nonplanar polycrystalline SiGe thermal microemitters for infrared dynamic scene projection
Appl. Phys. Lett. **94**, 213514 (2009); 10.1063/1.3148645

Surface-emitting terahertz quantum cascade laser source based on intracavity difference-frequency generation
Appl. Phys. Lett. **93**, 161110 (2008); 10.1063/1.3009198

Highly coherent thermal emission obtained by plasmonic bandgap structures
Appl. Phys. Lett. **92**, 081913 (2008); 10.1063/1.2883948

Coherent near-infrared wavelength conversion in semiconductor quantum cascade lasers
Appl. Phys. Lett. **89**, 183507 (2006); 10.1063/1.2374842

Generation of coherent terahertz radiation with multifrequency modes in a Fibonacci optical superlattice
Appl. Phys. Lett. **83**, 1071 (2003); 10.1063/1.1598644

AIP | APL Photonics

APL Photonics is pleased to announce
Benjamin Eggleton as its Editor-in-Chief

[This article is copyrighted as indicated in the article. Reuse of AIP content is subject to the terms at: http://scitation.aip.org/termsconditions. Downloaded to] IP: 149.151.178.171 On: Thu, 24 Sep 2015 20:07:04

Ab initio design of coherent thermal sources

Jérémie Drevillon and Philippe Ben-Abdallah[a)]
Laboratoire de Thermocinétique, CNRS UMR 6607, Ecole Polytechnique de l'Université de Nantes, 44 306 Nantes Cedex 03, France

(Received 6 June 2007; accepted 26 September 2007; published online 6 December 2007)

Emission of thermal light from a hot body has been considered for a long time as broadband and quasi-isotropic. Today, we know that this paradigm is wrong and it has been shown that many micro- and nanostructured materials are able to radiate in narrow spectral bands and around specific directions of space. However, so far, only heuristic strategies based on trial and error have been followed for engineering such sources. Here, we present a general method for the *ab initio* design of coherent thermal sources by using only the first principles of optics. Our results pave the way toward the inverse design of new composite emitting structures for high performance applications in optics. © *2007 American Institute of Physics*. [DOI: 10.1063/1.2816244]

I. INTRODUCTION

Functional nanomaterials offer a unique opportunity to make breakthrough discoveries and truly revolutionary developments that are needed to succeed the energy challenge. The density functional theory developed by Kohn and Sham[1] in the mid-60s has opened the way by circumventing many difficulties of quantum framework to the inverse design of nanostructured functional materials from the first principles of physics. However, up to now, the *ab initio* design has mainly been applied to the development of new materials with specific electronics, spintronics, and magnetic properties.[2] In the present work, we make a step toward the inverse design of functional materials for infrared optics. We report numerical experimentations demonstrating that it is possible to predict the inner structure of nanolayered thermal sources for controlling both spatially and spectrally their emission, reflection, and transmission properties. To date, a large number of micro- and nanostructured materials such as surface relief gratings,[3,4] photonic crystals,[5–7] vertical cavities and planar multiplayer structures,[8–11] metamaterials,[12,13] and even hybrid structures[14] have been synthesized to this end. However, all these nanostructured materials have been designed following a basic trial-and-error approach rather than a more rational bottom-up method. The ability to artificially grow in a controllable manner, from modern deposition techniques, complex structural configurations of metallic, polar, and dielectric materials raises now the issue of the "best" achievable inner structures to tailor the radiative properties of a nanostructured thermal source in a prescribed manner and to enhance the coherence degree of its emission. Until now, this engineering design problem was remained an open problem. Here, we introduce the first method for a rational design of multilayered functional materials for infrared optics. Our approach is based only on the basic principles of optics that is on the photon wave equation or its equivalent optical network for one-dimensional structures and needs only the dielectric and magnetic properties of materials as entrance parameters.

II. RADIATIVE PROPERTIES OF A PLANAR MULTILAYER STRUCTURE

The structures investigated in this paper are shown in Fig. 1. They are one-dimensional stacks built by superposing nanolayers of different dielectric materials. All these composite materials are formed from M unit nanolayers of the same total thickness L. Each layer is either an emitting (lossy) or a nonemitting (transparent) material in the region of infrared spectrum under investigation. We remind hereafter the basis principles for the calculation of the spectral and directional emissivity $\varepsilon(\lambda,\theta)$, reflectivity $r(\lambda,\theta)$, and transmittivity $t(\lambda,\theta)$ of this structure. These radiative properties are readily evaluated from the transfer matrix $\mathbf{T}(0,L)$ of the

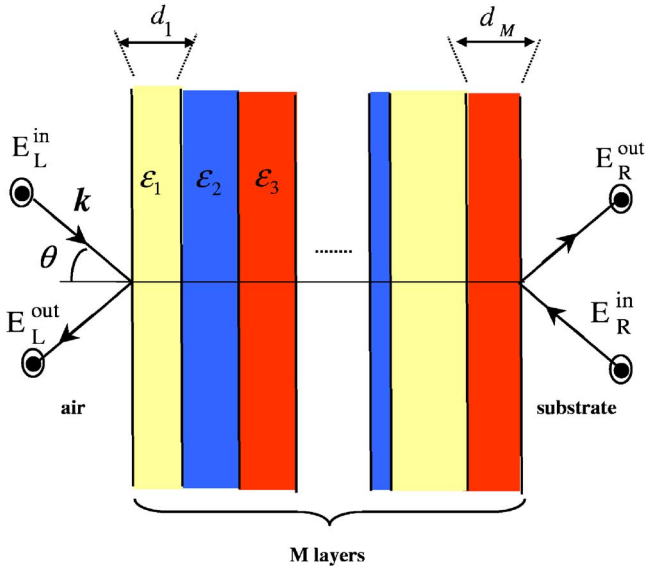

FIG. 1. (Color online) Schematic of the planar structure made of M layers of linear dielectric coated on a semi-infinite substrate. The electric field $\boldsymbol{E_L}=(E_L^{\text{in}},E_L^{\text{out}})$ on the left-hand side of the structure is linearly related to the electric field $\boldsymbol{E_R}=(E_R^{\text{out}},E_R^{\text{in}})$ on the right-hand side (here, only the scattering of TE waves is illustrated. **k** represents the wave vector of the incident field).

a)Author to whom correspondence should be addressed. Electronic mails: pba@univ-nantes.fr and philippe.benabdallah@polytech.univ-nantes.fr.

 © 2007 American Institute of Physics

[This article is copyrighted as indicated in the article. Reuse of AIP content is subject to the terms at: http://scitation.aip.org/termsconditions. Downloaded to] IP: 149.151.178.171 On: Thu, 24 Sep 2015 20:07:04

whole structure for both polarization states of light. True to the signature of corresponding optical network, this matrix relates the electric field $|\boldsymbol{E_L}\rangle=(E_L^{\text{in}},E_L^{\text{out}})$ on the left-hand side of the structure to the field $|\boldsymbol{E_R}\rangle=(E_R^{\text{out}},E_R^{\text{in}})$ on its right-hand side by a relation of the form $|\boldsymbol{E_L}\rangle=\mathbf{T}(0,L)|\boldsymbol{E_R}\rangle$. This matricial relation is perfectly well adapted to the composition of elementary networks corresponding to a piling up process. Thus, the transfer matrix of the whole structure is the result of product $\mathbf{T}(0,L)=\Pi_{i=1}^{M}\mathbf{T}_{\text{sub}}(i)$ of elementary transfer matrix $\mathbf{T}_{\text{sub}}(i)$, which describes either the traversal of an interface between two media

$$T_{\text{sub}}=\frac{1}{t_{ij}}\begin{pmatrix}1 & r_{ij}\\ r_{ij} & 1\end{pmatrix} \tag{1a}$$

or the phase shift of field across a layer

$$T_{\text{sub}}=\begin{pmatrix}e^{i\phi_j} & 0\\ 0 & e^{-i\phi_j}\end{pmatrix}. \tag{1b}$$

Here, t_{ij} and r_{ij} are the transmission and reflection Fresnel coefficients,[15] respectively, at the interface between the medium i and the medium j and ϕ_j stands for the phase shift of waves across the layer j. It follows that the spectral and directional transmitivity $t(\lambda,\theta)$ and reflectivity $r(\lambda,\theta)$ of a structure are given in terms of transfer matrix components by $t=|E_R^{\text{out}}/E_L^{\text{in}}|^2=|1/T_{11}|^2$ and $r=|E_L^{\text{out}}/E_L^{\text{in}}|^2=|T_{21}/T_{11}|^2$. Moreover, from Kirchoff's law, we know that the directional (polarized) and spectral emissivity $\varepsilon(\lambda,\theta)$ is given by $\varepsilon=\alpha=1-t-r$, where α denotes the absorptivity of the structure. It is important to outline that all internal multireflection and reabsorption effects within and between each layer are included in the formalism of transfer matrix. Detailed discussions about the matrix transfer theory and its numerical stability can be found in Ref. 15.

III. RATIONAL DESIGN OF SOURCES

The total number of all possible configurations that can be theoretically fabricated with N distinct materials is N^M. For binary structures made with 100 unit layers, there are more than 10^{30} possible configurations. It will be as great as 10^{47} for three basis materials. Such a large space offers immense possibilities to sculpt the radiative properties of nanolayered composites. However, to explore effectively this vast space of composite materials and identify the structures which possess the desired properties, a rational searching method is needed. To do that, we use a genetic algorithm[16] (GA) which is a stochastic global optimization method based on natural selection rules in a similar way to Darwin's theory of evolution. The main steps of GA are summarized hereafter. Step 1: The evolution process is started by generating an initial generation also called population (typically few tens to 1000) of random structures. In parallel, we define some target radiative properties [for instance, the spectral and directional emissivity $\varepsilon_{\text{target}}(\lambda,\theta)$ and reflectivity $r_{\text{target}}(\lambda,\theta)$] that we want to recover. Then, in order to select the best morphologies in this population, in comparison with these objectives functions, we calculate the radiative properties [transmittivity $t(\lambda,\theta)$, reflectivity $r(\lambda,\theta)$, and emissivity $\varepsilon(\lambda,\theta)$] of each invidious by using their transfer matrix. Step 2: The discrepancy between these targets and the radiative properties of current structures is measured by a fitness function under the form

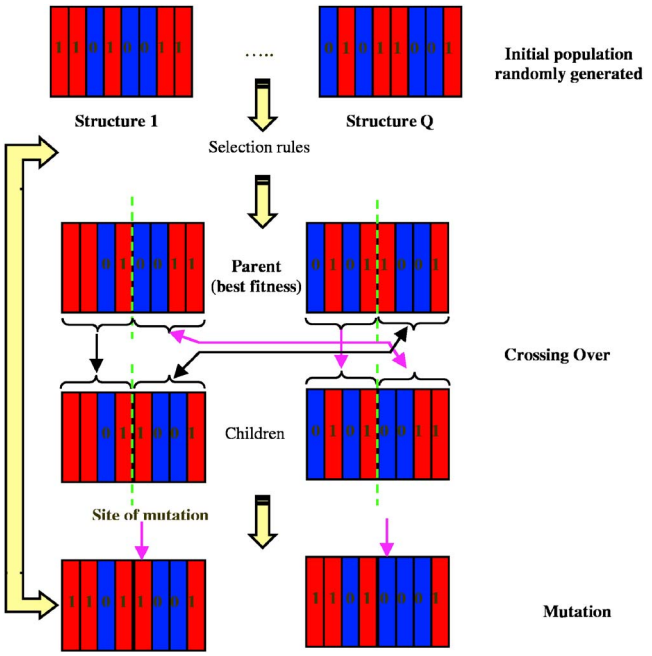

FIG. 2. (Color online) Principle of genetic algorithm (GA) used to design a binary nanostructured one-dimensional functional material. Here, the main steps of GA are described: initialization of a random population, selection of parents generation, cross over, and mutation.

$$J=\sum_p\int_{\theta_1}^{\theta_2}\int_{\lambda_{\min}}^{\lambda_{\max}}[\varepsilon_{\text{target}}(\lambda,\theta)-\varepsilon_{\text{calc}}^p(\lambda,\theta)]^2d\theta d\lambda + \sum_p\int_{\theta_1}^{\theta_2}\int_{\lambda_{\min}}^{\lambda_{\max}}[r_{\text{target}}(\lambda,\theta)-r_{\text{calc}}^p(\lambda,\theta)]^2d\theta d\lambda, \tag{2}$$

where the discrete sum operates over both states of polarization of the thermal light. Step 3: Once the fitness has been calculated, some population's members are selected on the basis of their fitness function to become parents and to produce children structures in a breeding procedure known as crossover (Fig. 2). One of most natural selection rule is to keep only for the next generations the structures with a fitness function below a threshold. The crossover involves the creation of two children structures which are a combination of structural features of their parents. For example, by applying a simple one point crossover technique for binary structures, the parents 110010011 and **01011001** are split and recombined to form two children structures 11001**1001** and **0101**0011. Step 4: Some mutations are involved in the children's generation to improve the performances of the algorithm and avoid converging toward local minima. To do that, we generate a random variable p_m which defined the probability for an arbitrary cell in a structure at the mth generation to be changed. This step is fundamental to maintain a certain diversity in the children generation. When p_m is large, the evolution algorithm tends to search randomly over the discrete space of all possible structures and the population members remain far from the best structure. In contrast,

[This article is copyrighted as indicated in the article. Reuse of AIP content is subject to the terms at: http://scitation.aip.org/termsconditions. Downloaded to] IP: 149.151.178.171 On: Thu, 24 Sep 2015 20:07:04

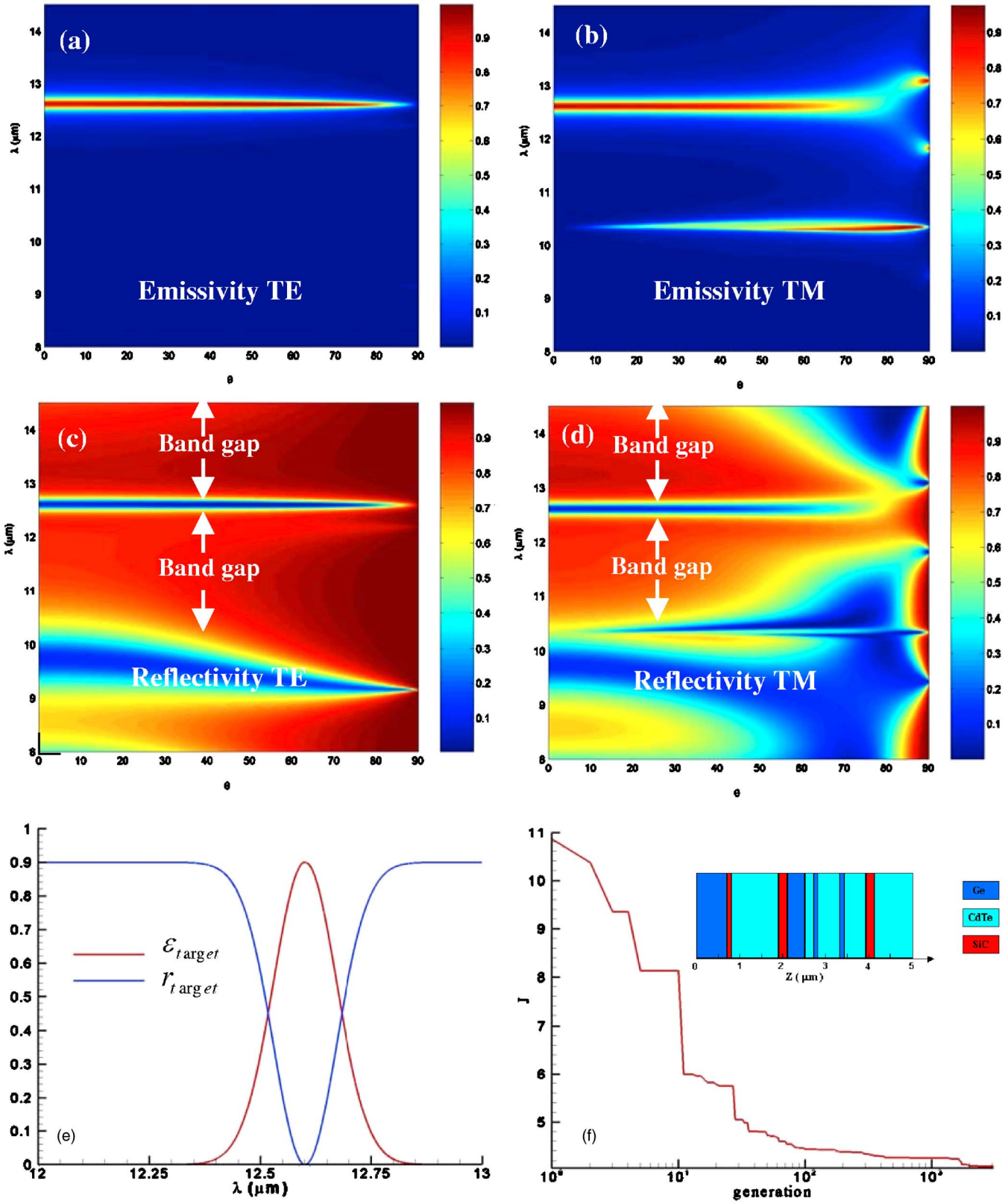

FIG. 3. (Color online) Spectral and directional emissivity [(a) and (b)] and reflectivity [(c) and (d)] of a quasimonochromatic thermal source made with 50 nanolayers of SiC, Ge, and CdTe 100 nm thick and designed by GA. The peak of emission which appears at $\lambda=10.4$ μm in polarization TM at oblique incidence is outside of minimization domain $[\lambda_{min};\lambda_{max}]$. (e) Target radiative properties. (f) Fitness function ($\times 0.001$) vs the generation number and structure of the designed source. GA parameters: $\lambda_{min}=12.2$ μm, $\lambda_{max}=12.8$ μm, $\theta_{min}=0°$, $\theta_{max}=80°$, and $m=3100$. The mutation probability is adjusted according to relation (3), each $I=10$ generations.

when p_m is small, the searching algorithm tends to the nearest local extremum. Thus, an appropriate choice of p_m is crucial for balancing the local convergence and the global search. To keep this mutation efficient, we furthermore adjust p_m to each I generation according to the following incrementing rule:

[This article is copyrighted as indicated in the article. Reuse of AIP content is subject to the terms at: http://scitation.aip.org/termsconditions. Downloaded to] IP: 149.151.178.171 On: Thu, 24 Sep 2015 20:07:04

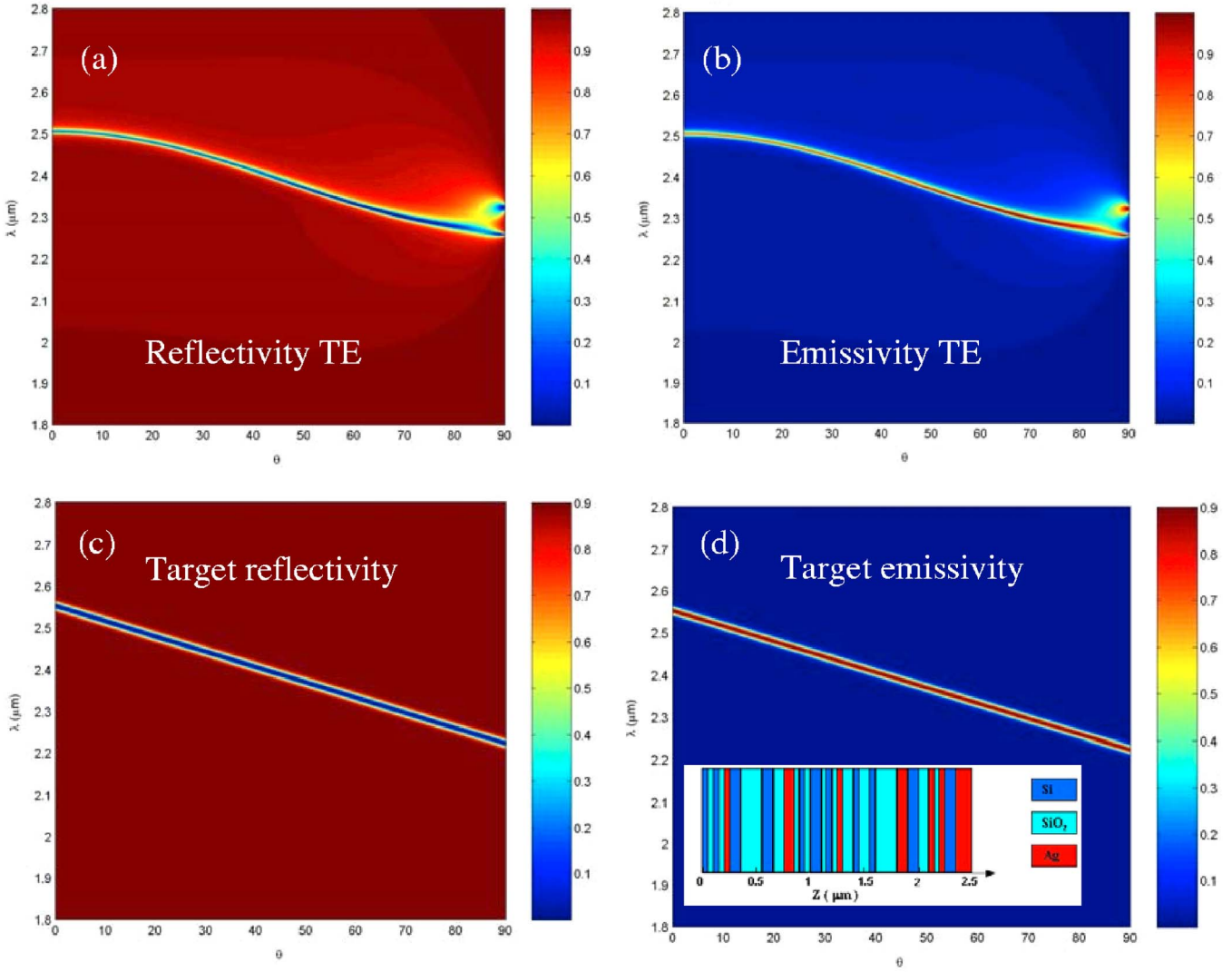

FIG. 4. (Color online) Spectral and directional (a) reflectivity and (b) emissivity in polarization TE of a partially coherent thermal source made with 50 nanolayers of Ag, Si, and SiO_2 layers 50 nm thick and designed by GA. [(c) and (d)] Target radiative properties and structure of the designed source (inset of d). GA parameters: $\lambda_{min}=1.8$ μm, $\lambda_{max}=2.8$ μm, $\theta_{min}=0°$, $\theta_{max}=90°$, and $m=200$. The mutation probability is adjusted according to relation (3), each $I=10$ generations.

$$\Delta p_m = \begin{cases} +\xi, & \gamma < 1/3 \\ 0, & 1/3 < \gamma < 2/3 \\ -\xi, & \gamma > 2/3, \end{cases} \tag{3}$$

where ξ denotes the change of mutation probability and γ is the ratio of the averaged fit over the current population to the minimal fit. Then, we introduce some new structures randomly designed to keep the same total number of structures in every population. This operation introduces diversity throughout the evolution process. Finally, we select new parent structures among this children population and go back to the selection step and so on until an optimal structure is found.

IV. QUASIMONOCHROMATIC AND ISOTROPIC THERMAL SOURCE

We present here two nanostructured thermal sources that we have designed following the rational approach described above. The first one is a quasi-isotropic and isotropic source that has been imagined to radiate in a narrow spectral band (Fig. 3) over any direction of space. To synthesize this source, we adopt a ternary structure consisting of silicium carbide (SiC), germanium (Ge), and telluride cadmium (CdTe) layers. This source is designed to operate in the range of wavelength (8 μm; 14.5 μm). In this region, both Ge and CdTe are transparent materials and their dielectric permittivities can be approximated[17] by the constant values $\tilde{\varepsilon}_{Ge}=16$ and $\tilde{\varepsilon}_{CdTe}=7.29$. As for the SiC, it is the only dissipative material and its dielectric function is correctly described by the simple oscillating Lorentz model[17] $\tilde{\varepsilon}_{SiC}=\tilde{\varepsilon}_{\infty}[1+(\omega_L^2-\omega_T^2/\omega_T^2-\omega^2-i\Gamma\omega)]$, where $\omega_L=18.253\times10^{13}$ rad s^{-1}, $\omega_T=14.937\times10^{13}$ rad s^{-1}, $\Gamma=8.966\times10^{11}$ rad s^{-1}, and $\tilde{\varepsilon}_{\infty}=6.7$ denote the longitudinal and transversal optical phonon pulsation, the damping factor, and the high frequency dielectric constant, respectively. Moreover, all materials involved here are nonmagnetic in this wavelength range. As target emissivity, we choose the Gaussian function $\varepsilon_{target}=\varepsilon_{max}\times\exp[-Q^2\ln 16(\lambda-\lambda^*)^2/\lambda^{*2}]$, which is centered at $\lambda^*=12.6$ μm, the wavelength of upper edge of the phonons

[This article is copyrighted as indicated in the article. Reuse of AIP content is subject to the terms at: http://scitation.aip.org/termsconditions. Downloaded to] IP: 149.151.178.171 On: Thu, 24 Sep 2015 20:07:04

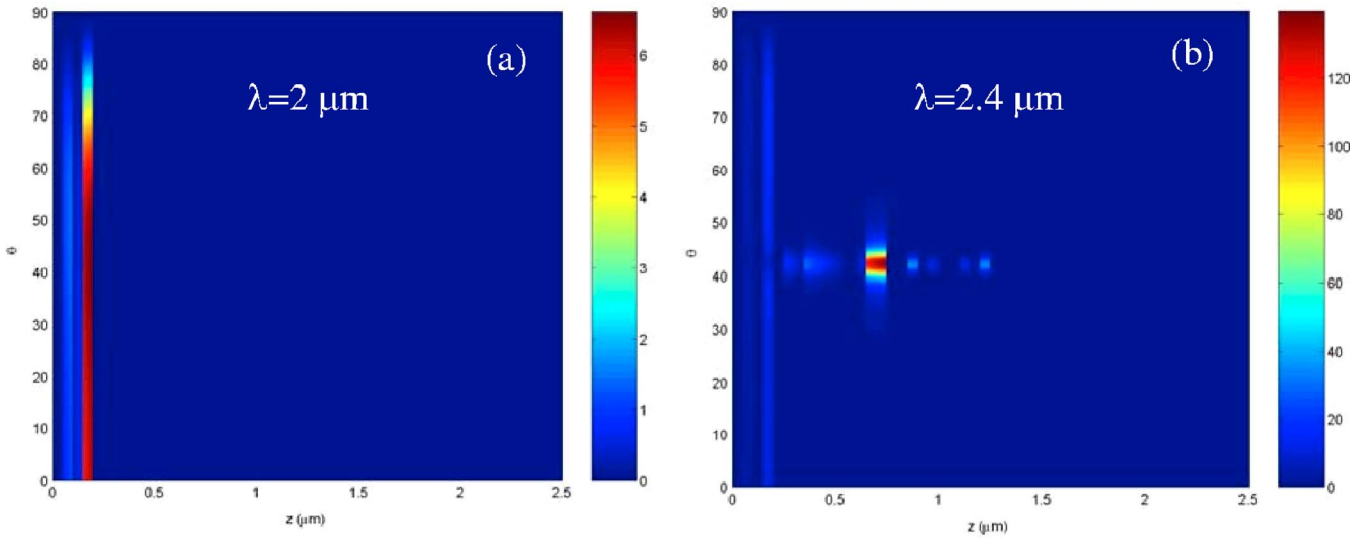

FIG. 5. (Color online) Modulus of the electric field (polarization TE) inside the inverse designed metallodielectric structure when it is highlighted by an incoming field of unit magnitude. Wavelengths of excitation are (a) $\lambda=2$ μm and (b) $\lambda=2.4$ μm. In (b), the strong intensity of field at $z=750$ nm around 42° demonstrates the presence of a resonant coupling between the incident (propagative) wave and the surface (evanescent) waves supported by the metallic layer at this position. This resonance coincides with the emission peak observed in Fig. 4 at 42° when $\lambda=2.4$ μm. Also, a weak coupling between the surface plasmons and the incident wave is observed in (a) and (b) at $z=200$ nm. However, the comparison between Figs. 4 and 5 shows that the transfer of energy from photons to electrons in this region is too small to significantly participate to the thermal emission of the structure.

absorption band in SiC [in the neighborhood of a resonant wavelength (real part of the complex pole of the emissivity), the emissivity curve can be well approximated by a Gaussian (see, for instance, Petit in Ref. 18)]. At this wavelength, the SiC layers support evanescent modes regardless of the angle of incidence so that when these localized waves are excited from an external perturbation, the incident energy is resonantly transferred to SiC phonons and causes a large absorption of light. In accordance with Kirchoff's law,[19] this photon-photon coupling supports a strong emission at the same wavelength. Also, in order to use the structure as coating material, we set a target reflectivity under the form $r_{\text{target}}=1-t_{\text{target}}-\varepsilon_{\text{target}}$, where $t_{\text{target}}\ll 1$ which allows only the thermal light close to λ^* to be transferred to the multilayered source from an eventual substrate, all the rest light being back reflected. The degree of spectral coherence[18] of this source, measured by its quality factor $Q=\lambda^*/\Delta\lambda$, namely, the ratio of the resonance wavelength over the full width at half maximum of the resonance, is set to 80, while the maximum of emissivity searched is $\varepsilon_{\max}=0.95$. For the present structure, we use the following geometric parameters: $M=50$ and $d=L/M=100$ nm. As for the fitness, it is minimized over the spectral range ($\lambda_{\min}=12.2$ μm; $\lambda_{\max}=12.8$ μm) and the angular domain ($\theta_1=0$; $\theta_2=80°$). Figure 3(f) shows the designed structure obtained after $m=3100$ generations. One can see that the structure produced by *ab initio* design is highly disordered and very difficult to intuit *a priori*. Its reflectivity pattern plotted over the enlarged spectral range (8 μm; 14.5 μm) shows the presence, out of λ^*, of a large and quasicomplete (omnidirectional) band gap (except at oblique incidences) in the spectral range (11 μm; 14 μm). So far, such omnidirectional band gaps had been observed only in periodic and quasiperiodic materials such as photonic crystals[5] and quasicrystals.[20–22] This band gap is clearly desirable in the perspective of using this nanostructure as coating material. As for the emission spectrum, it is quasiresonant ($\varepsilon\approx\varepsilon_{\max}$) precisely at λ^* in this band gap for almost every direction of space. Hence, the designed structure can be interpreted as a phonon-polariton resonant guide. Indeed, it behaves like a mirror in the band gap and converts any photon into atomic vibration (phonons) at λ^* by resonant photon-phonon coupling.

V. PARTIALLY COHERENT INFRARED SOURCE

The second structure we have inversely designed is a multilayered plasmonic structure made with silver (Ag), silicon (Si), and glass (SiO_2) layers that exhibit both partial spatial and spectral coherence. Contrary to the first source, our goal here is to control the thermal emission not only in frequency but also in direction. The target emissivity and reflectivity plotted in Fig. 4 are defined in the spectral range ($\lambda_{\min}=1.8$ μm; $\lambda_{\max}=2.8$ μm) where Ag supports surface waves also called as surface plasmon (SP). These waves are due to collective motion of electrons in Ag. In this spectral range, the dielectric permittivities of Si and SiO_2 are well approximated[19] by the real values $\tilde{\varepsilon}_{\text{Si}}=11.15$ and $\tilde{\varepsilon}_{\text{SiO}_2}=2.1025$, while the Ag permittivity is complex valued and described by the free electron/Drude model $\tilde{\varepsilon}_{\text{Ag}}=1-[\omega_p^2/\omega(\omega-i\omega_c)]$, where $\omega_p=13.69\times10^{15}$ rad s^{-1} is the plasma pulsation and $\omega_c=2.73\times10^{13}$ rad s^{-1} is the electron collision frequency. The geometric parameters of the studied structure have been set to $M=50$, and $d=50$ nm. Figure 4 shows that the targets are relatively well recovered for both polarization states (only TE polarization is plotted) with an evolution process of 200 generations only. Once again the structure is highly disordered. As for the quality factor, it reaches ~238 at normal incidence and falls to about 200 at 60°. These values are the highest values reported so far with planar multilayer structures using Ag films.

[This article is copyrighted as indicated in the article. Reuse of AIP content is subject to the terms at: http://scitation.aip.org/termsconditions. Downloaded to] IP: 149.151.178.171 On: Thu, 24 Sep 2015 20:07:04

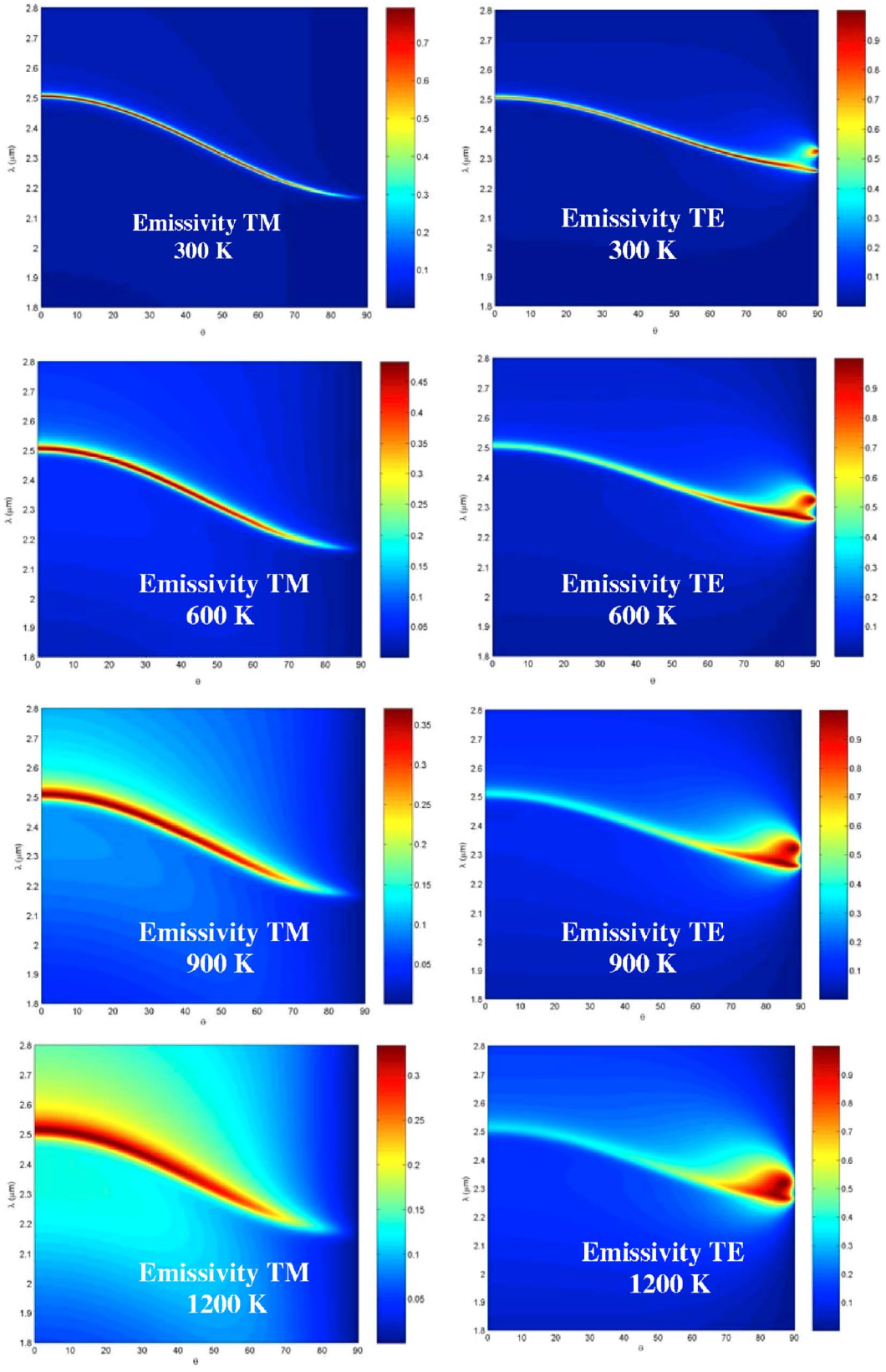

FIG. 6. (Color online) Thermal dependence of the emissivity spectrum in polarizations TM and TE of a partially coherent thermal source made with 50 nanolayers of Ag, Si, and SiO_2 layers 50 nm thick and designed by GA (see Fig. 4).

In order to find the physical origin of the partially coherent emission, we now examine the field inside the designed structure (see Appendix) when it is submitted to external (unit) excitations. The result displayed in Fig. 5 shows that the intensity of electric field inside the structure becomes locally much larger than one at the incidence angles and wavelengths where the emissivity pattern is maximum. As we can see on this figure, this is due to internal resonant

[This article is copyrighted as indicated in the article. Reuse of AIP content is subject to the terms at: http://scitation.aip.org/termsconditions. Downloaded to] IP: 149.151.178.171 On: Thu, 24 Sep 2015 20:07:04

mechanisms. Indeed, if we pay attention on the case where an incident wave of wavelength $\lambda=2.4\ \mu$m impinges the structure under an angle of 42°, we observe that the field at the interface between the Ag and SiO_2 layers at $z=0.75\ \mu$m is strongly enhanced by more than two orders of magnitude. Such a resonance, exponentially localized on both sides of the Ag layer, reveals the presence of a SP and demonstrates that the incident wave is able to couple with it. Thus, the energy of this propagative wave is resonantly transferred to SPs. Therefore, this coupling directly contributes to the strong emission of the structure in the angular lobe centered at 42°. In contrast, for all other angles of incidence at the same frequency and for all angles outside of the range $(2.25\ \mu\text{m};2.55\ \mu\text{m})$, there is no significant enhancement of field in the structure and very few energy is absorbed by the Ag layers. Then, according to Kirchoff's law, the thermal emission of the structure is very small.

Until now, we have not studied the influence of the temperature dependence of optical properties on the emission spectrum of the source. Here, we examine in the extent that the temperature field is able to affect the coherence degree of the source designed. To describe the temperature dependence of silver permittivity, we use the following model (see Celanovic *et al.*[11] and Refs. 20 and 21 therein):

$$\omega_c(T)=\left[\frac{\omega_c(T=300\ \text{K})^{1.3}}{300}\right]T^{1.3}, \tag{4}$$

while the optical properties of glass and silicium are assumed to remain constant over the temperature range that we investigate $(T=300\ \text{K};T=1200\ \text{K})$. According to relation (4), an increase in temperature causes a shift in the electron collision frequency toward the high frequencies and thus, an increase of the photon absorption at short wavelength in the metal. Accordingly, we see in Fig. 6 that the emissivity of the structure decreases as the temperature increases for both polarization states. We also observe that the peak of emission spreads as the temperature increases and the magnitude of emission strongly decreases. This means that the spectral coherence of the source is altered at high temperature. Indeed, in this case the coupling of incident wave with the silver's SPs is less strong. For TE waves, the peak of emission becomes more and more localized around the tangential direction due to the presence of surface plasmon modes supported by the silver layers.

VI. CONCLUSION

The present work has demonstrated the feasibility and efficiency of *ab initio* design for infrared optics. The approach developed in this work is very promising to improve the performance of numerous optical technologies such as photovoltaic and thermophotovoltaic cells, spectroscopy, and chemical sensing. It opens interesting insight for the development of new materials such as superlens for nanoscale imaging or nanolitography. Also, the rational design of materials should find numerous ramification and applications in other fields of physics. For instance, it should allow us to sculpt the transport properties of nanocomposite materials by considering their energy carriers (electrons, photon, phonons, magnons, excitons, etc.) as waves moving in a scattering network. In particular, our work opens interesting prospects for thermoelectric conversion by providing a method to achieve materials with high figure of merit, that is, with high electric conductivity and small thermal conductivity.

ACKNOWLEDGMENTS

This work was supported by an ESTEC/European Space Agency Grant No. 20270/06/NL/HE.

APPENDIX: RESPONSE TO A UNIT ELECTRIC FIELD IN A MULTILAYERED STACK

The electric field distribution within the structure when it is highlighted by an incoming field of unit magnitude is calculated using the reflectivity coefficient r of the whole structure and the partial transfer matrix $\mathfrak{I}=\boldsymbol{T}(0,z)$ from the highlighted side (here, located at $z=0$) and the current point. It is straightforward to see that the local field is given by $E(z,\theta,\lambda)=[\mathfrak{I}_{22}+\mathfrak{I}_{21}-r(\lambda,\theta)(\mathfrak{I}_{11}+\mathfrak{I}_{12})]/\det\mathfrak{I}$. Its intensity is then simply the square of this expression, as plotted in Fig. 5. We see that in some regions, this intensity becomes significantly larger than one due to internal resonance phenomena. These resonances reveal the presence of couplings between localized (evanescent) modes and the incident (propagative) wave. When this mechanism takes place in a lossy material, it enhances the absorption process at the frequency of localized modes and magnifies the thermal emission.

[1]W. Kohn and L. J. Sham, Phys. Rev. **140**, 1133 (1965).
[2]L. Niebergall, V. S. Stepanyuk, J. Berakdar, and P. Bruno, Phys. Rev. Lett. **96**, 127204 (2006); see also H. Katayama-Yoshida and K. Sato, Physica B **327**, 337 (2007).
[3]H. Sai, H. Yugami, Y. Akiyama, Y. Kanamori, and K. Hane, J. Opt. Soc. Am. A **18**, 1471–1476 (2001).
[4]J. J. Greffet, R. Carminati, K. Joulain, J. P. Mulet, S. Mainguy, and Y. Chen, Nature (London) **416**, 61 (2002).
[5]S. John, Phys. Rev. Lett. **58**, 2486 (1987); also, see E. Yablonovitch, Phys. Rev. Lett. **58**, 2059 (1987); for a more recent review, see H. Benisty, S. Kawakami, D. Norris, and C. Soukoulis, Photonics Nanostruct. Fundam. Appl. **2**, 57 (2004).
[6]M. U. Pralle, N. Moelders, M. P. McNeal, I. Puscasu, A. C. Greenwald, J. T. Daly, E. A. Johnson, T. George, D. S. Choi, I. El-Kady, and R. Biswas, Appl. Phys. Lett. **81**, 4685 (2002).
[7]L. McCall, P. M. Platzman, R. Dalichaouch, D. Smith, and S. Schultz, Phys. Rev. Lett. **67**, 2017 (1991); E. Yablonovitch, T. J. Gmitter, and K. M. Leung, *ibid.* **67**, 3380 (1991).
[8]P. Ben-Abdallah and B. Ni, J. Appl. Phys. **97**, 104910 (2005).
[9]B. J. Lee, C. J. Fu, and Z. M. Zhang, Appl. Phys. Lett. **87**, 071904 (2005); see also C. J. Fu, Z. M. Zhang, and D. B. Tanner, Opt. Lett. **30**, 1873 (2005).
[10]P. Ben-Abdallah, J. Opt. Soc. Am. A **21**, 1368 (2004).
[11]B. J. Lee and Z. M. Zhang, J. Appl. Phys. **100**, 063529 (2006); see also I. Celanovic, D. Perreault, and J. Kassakian, Phys. Rev. B **72**, 075127 (2005), and references therein.
[12]S. Enoch, G. Tayeb, P. Sabouroux, N. Guérin, and P. Vincent, Phys. Rev. Lett. **89**, 213902 (2002).
[13]S. Zhang, W. Fan, B. K. Minhas, A. Frauenglass, K. J. Malloy, and S. R. J. Brueck, Phys. Rev. Lett. **94**, 037402 (2005); **95**, 137404 (2005).
[14]A. Battula and S. C. Chen, Phys. Rev. B **74**, 245407 (2006); see also M.-W. Tsai, Appl. Phys. Lett. **89**, 173116 (2006).
[15]P. Yeh, *Optical Waves in Layered Media* (Wiley, New York, 1988).
[16]J. H. Holland, *Adaptation in Natural and Artificial Systems* (MIT Bradford Books Edition, Cambridge, MA, 1992).
[17]E. D. Palik, *Handbook of Optical Constants of Solids* (Academic, London 1998).
[18]L. Mandel and E. Wolf, *Optical Coherence and Quantum Optics* (Cambridge University Press, New York, 1995); see also R. Petit, *Electromagnetic Theory of Gratings* (Springer-Verlag, Berlin, 1980).

[This article is copyrighted as indicated in the article. Reuse of AIP content is subject to the terms at: http://scitation.aip.org/termsconditions. Downloaded to] IP: 149.151.178.171 On: Thu, 24 Sep 2015 20:07:04

[19]M. F. Modest, *Radiative Heat Transfer* (McGraw-Hill, New York, 1993).
[20]W. Gellermann, M. Kohmoto, B. Sutherland, and P. C. Taylor, Phys. Rev. Lett. **72**, 633 (1994).
[21]T. Hattori, N. Tsurumachi, S. Kawato, and H. Nakatsuka, Phys. Rev. B **50**, 4220 (1994).
[22]A. Della Villa, S. Enoch, G. Tayeb, V. Pierro, V. Galdi, and F. Capolino, Phys. Rev. Lett. **94**, 183903 (2005), and references therein.

[This article is copyrighted as indicated in the article. Reuse of AIP content is subject to the terms at: http://scitation.aip.org/termsconditions. Downloaded to] IP: 149.151.178.171 On: Thu, 24 Sep 2015 20:07:04